PAPER • OPEN ACCESS

Prediction of an advanced spar's horizontal motions, validated by full scale observation data

View the article online for updates and enhancements.

Prediction of an advanced spar's horizontal motions, validated by full scale observation data

Haruki Yoshimoto[1], Christopher Wright[2], Ryota Wada[2] and Ken Takagi[2]

[1]Japan Marine United Corporation, Yokohama-City, Kanagawa, Japan.
[2]The University of Tokyo, Tokyo, Japan.

E-mail: `wrightc@edu.k.u-tokyo.ac.jp`

Abstract. As the offshore wind industry moves into deeper waters, the number of different floating wind platform concepts continues to expand. Accurately predicting the motion characteristics of these novel platforms is crucial to the safe and economic conversion of wind energy into electricity. A challenge in the currently used numerical simulation methods involves successfully predicting the slow drift motions and damping, especially in complex realistic environmental conditions which include multi-directional spectral waves, current and wind loading. Of most uncertainty to these predictions is determining the low frequency viscous damping which dominates the resonant surge and sway motions. In this paper, full-scale motion observations of the Fukushima FORWARD's floating wind substation are used to determine the platforms viscous drag forces. These drag coefficients are used in a combined potential flow and Morison's equation model to capture the observed behaviour. This validated numerical model is then used to describe the required fidelity of mooring line models, in order to aid platform developers in the early stages of design.

1. Introduction

As the offshore wind energy industry moves into deeper waters, floating platforms for supporting wind turbines are being proposed, developed and installed as the solution. There are numerous designs for floating structures in all stages of design, from conceptualisation to full scale deployment, with vastly different design characteristics, however these platform types can be generally categorised by how the primary stability mechanism is achieved. Spar buoys achieve stability through counter weight ballast, semi-submersibles through water plan area righting moment and tension leg platforms through excess buoyancy providing pretension in the mooring lines. From these primary categories there can be numerous sub categories, for example spar platforms can be mono-column, advanced spar, truss spar or pendulum spar amongst others. Each type has a number of unique attributes and as the floating wind industry platform designers have not converged to a single type, there is also much research into the benefits and challenges of each.

This research concentrates on the main horizontal motions of advanced spar type platforms (surge and sway, as yaw motion is negligible). Horizontal motions are excited by wind, wave and current and dominate the design of mooring systems. Limits on horizontal motions are also required to ensure the safe operations of power umbilical cables connecting floating wind turbines (FWTs) to the wind farm grid system. For mooring system and power umbilical design,

accurately predicting the horizontal motions is crucial. As platforms horizontal (surge and sway) natural frequencies are commonly much below the wave excitation frequencies, it is second order wave, wind and current which provide the excitation forces. Low frequency damping is a combination of wave drift damping, floater viscous damping, mooring and umbilical line damping, current, wind and radiated wave damping. Large amplitude slow drift oscillations are known to make the viscous flow separation more significant compared to the small oscillation wave frequency oscillations [1]. The authors previous research [2] on an advanced spars platform's low frequency motion concluded that the viscous drag dominated the damping due to the platform geometry, and showed a tendency to increase with increasing wave severity. Common numerical modelling methods using potential flow theory neglect any viscous forces due to the assumptions that flow is inviscid and irrotational. Viscous forces are generally added to potential flow theory models in order to increase the accuracy of predictions made by those models, one such method is using only the drag component of Morison's equation [3]. Selection of the drag coefficients to use in drag force formulas is critical to the accurate use of such methods. Coefficients are generally selected from a combination of the following methods: the modeler's experience of similarly shaped offshore platforms, a literature review, scaled model experiments in wave basin tests, computational fluid dynamics or from full scale deployments. Each method has its own unique challenges, and consistency across methods varies. Drag coefficients are seen to vary between still water and across varying sea-states. Lemmer [4] showed through experimental testing and a reduced order numerical model of the tripple-spar floating wind turbine that the required drag coefficient reduces from 2.0 in still water to 0.8 and 0.6 with increasing wave severity. This inverse relationship between sea-state intensity and damping has been shown in other research, described as accounting for missing additional nonlinear wave excitation, which become more significant with increasing wave height [5]. Operational Modal Analysis (OMA) has also been successfully used to analyse the damping rates of floating wind turbines. Pegalajar [6] analysed experimental data of a semi-submersible FWT using OMA and found that the damping generally increased with increasing wave severity. Errors in surge and sway grew with increasing sea-states, likely due to a simplification of the second order quadratic transfer functions (QTF's) and neglecting a third order viscous mean drift force. The third order viscous mean drift force arises from integrating the viscous force up to the instantaneous free surface, or when the instantaneous floater position is used to apply the force [7].

Improvements to classic numerical modelling techniques have also been proposed and verified in recent years. For example using frequency dependent hydrodynamic parameters in Morison's equation type models [8]. Stansberg [9] found interaction effects between wave and current forces on wave drift motions and proposed an empirical correction factor to improve potential flow models. When compared against tank testing of a semi-submersible platform this correction led to good estimates of slow drift motions. The empirical correction factor has been generalised to include the effects of non-collinear waves and current [10] and has further tank testing validations [11] which indicate that the damping increases with increasing wave heights. Compared to the calm water damping, the low frequency surge damping in waves increases between 60 and 80 % for moderate and severe sea states without current and around 50 % for the checked severe sea state with current.

Validation of numerical modelling and design by full scale at sea observations is a vital aspect in furthering the understanding of hydrodynamics. Such validations has been undertaken historically on offshore oil and gas or purely experimental platforms, for example the Oryx Neptune Production Spar [12] or the POSEIDON experimental semi-submersible platform [13]. With the increased deployment of prototype offshore FWTs, there has been a recent interest in validating the modelling of these smaller more dynamic offshore platforms. For example the full-scale Hywind FWT was deployed off the coast of Norway in 2009 and showed that the motion characteristics could be accurately predicted using NREL's FAST software [14].

The floating substation of the Fukushima FORWARD floating wind farm has also been studied previously [2, 15, 16]. The 7MW Fukushima FORWARD V-shaped semi-submersible FWT has also been used for design and numerical modelling validation purposes [17, 18].

2. Objectives

In this paper the required viscous damping for the Fukushima FORWARD's floating substation is analysed. Numerical model drag coefficients are tuned to observation data from the full scale deployment across a range of sea-states. The required mooring model fidelity is also analysed. As computational expense increased with increasing mooring line fidelity these results are important for the use of early stage design tools.

3. Methodology

3.1. Numerical model

A numerical model is developed using combinations of the two software packages; ANSYS Aqwa and Orcina OrcaFlex. A detailed description of the model set up can be seen in [2]. Frequency domain hydrodynamic parameters are calculated using ANSYS Aqwa, which are then implemented into a time-domain numerical model developed in Orcina OrcaFlex. Viscous damping is applied using drag only Morison's equation elements as shown in Equation 1, where F_d. is the drag force, ρ is the density of sea-water, C_d. is the drag coefficient, A is the normal projected area and v_r. is the relative velocity between water particle and vessel. Although the platform is composed of octagonal hulls interconnected by cylindrical elements, in order to simplify the implementation of Morison's equation all elements are modelled as cylindrical elements of equal projected area in the normal direction. In order to account for the third order mean viscous drift force the viscous force is integrated to the instantaneous water line by means of Wheeler stretching [19]. The instantaneous vessel position is used to apply all forces including the drag force. The selection of the drag coefficients to implement is non trivial as seen in the author's previous publication on this platforms low frequency horizontal motions [2]. In order to best compare the varying simulation methods with the observed data, the drag coefficients for each individual sea-state are fitted. Details of this method are given in Section 3.2. Due to the small differences in results using Newman's formula for generating second-order forces over the more accurate full QTF method for wave heights as dealt with in the authors previous research [2], and the much quicker computational time, all simulations in this work use Newman's formula. For the mild to moderate sea-states used for this study the difference between low frequency surge and sway results using full QTF's and Newman's formula is less than 5%.

$$F_d = \frac{1}{2}\rho C_d A v_r |v_r| \tag{1}$$

Environmental force data includes a multi-directional wave spectra, discretized into 15 wave directions, a mean current velocity and direction, and a wind velocity time-series, all recorded on the observation platform. The original data groupings are used as in [2]. Two selection criteria are used to select which environmental cases to use. Firstly cases with a significant wave height above 2 m and a wind speed below 10 m/s, and secondly cases were selected with a significant wave height above 3.5 m without any wind speed limit. Current velocity was in the range of 0.1 to 0.6 m/s. Wind and current drag forces are calculated using the method outlined in [20] with the addition of the relative wind/current velocity between the platform and wind/current. Wind and current drag force coefficients were validated by prior experimental testing.

Modelling of mooring line is compared using the following methods, ranked in order of fidelity, with the highest first: 1) Finite-element model (FEM), 2) Analytic Catenary (AC) equations, 3) Nonlinear Catenary Spring, 4) Linear Spring. For 3) the Nonlinear Catenary Spring, the

horizontal force is the quasi-static restoring force as predicted by the FEM model. For 4) the Linear Spring, the force was linearised with the assumption of an extremely small offset. No vertical restoring forces are provided by either of the spring models. Only the FEM includes viscous damping induced by the motions of the mooring line. Mooring line drag coefficients are selected as 2.6 in the normal direction and 1.4 in the axial direction. A sensitivity study on mooring line drag damping showed the effects to be negligible in comparison with hull viscous damping. Mooring line damping can effect line tensions and has been used to tune numerical line tensions to experimental results in the past [21]. In the case of this work no observed line tensions are available so this was not considered further here. No additional damping to account for the loss of mooring line damping is added to the other methods. As both spring methods do not provide any of the additional weight that the catenary chain provides, an additional mass component equal to the submerged weight of the chains is added to the spar. For the "observed" line tensions, the motions of the platform are used to derive the line forces using the analytical catenary equations. No direct measurements of line tensions were undertaken during the observations, so this method is used to get the closest approximation. An attempt was made to use the platform motions coupled to a FEM mooring model, but noisy accelerations in the observed motion data, led to large inertial shock loads in the mooring system that were deemed to be unrealistic.

3.2. Tuning of drag coefficients to observed results

In this work the largest uncertainty involves a combination of the short term variability in the random wave seeds and the drag coefficients required to match the numerical models low frequency horizontal translations to the observation recordings. This section gives a description of how these are taken into consideration.

A single drag coefficient value is fitted to each of the observation data points. The square root of the variance of the low frequency surge and sway motions are used as the fit, as shown in eqn. 2 and as calculated spectrally by eqn. 3, where σ is the variance of motion, m_0 is the zeroth moment of the low frequency surge or sway motions, σ_X, σ_Y and σ_{XY} refer to the variance of the surge, sway and combined surge sway respectively, the subscripts $_{OBS}$ and $_{SIM}$ refer to observed and simulated results respectively. Low frequency motion is defined as that below 0.01 Hz. An iterative slope based approach is used to determine the next simulations drag coefficient, until a match to the observation data is found. Convergence here is denoted as a percentage error of less than 2.5% as shown in eqn. 4.

$$\sigma_{XY} = (\sigma_X^2 + \sigma_Y^2)^{0.5} \tag{2}$$

$$\sigma = m_0^{0.5} \tag{3}$$

$$\frac{\sigma_{XY,OBS} - \sigma_{XY,SIM}}{\sigma_{XY,OBS}} \leq \pm 0.025 \tag{4}$$

3.2.1. Short term variability in low frequency motions

As the observed wave recordings are of a spectral nature, no information exists about the exact wave time history. This presents a challenge to establishing the exact drag coefficients that are required to match the viscous damping in the numerical model with the observed data. An inherent short term variability exists in the simulated wave field due to the random wave phases applied to each wave component, this variability leads to variations in the simulated motions, particularly the low frequency motions, which are greatly affected by the exact wave train. As this work deals with numerical modelling validated by full scale observational data recorded at 20 minute, the standard simulation time

duration of 3 hours cannot be used. Recorded sea-state conditions are not stable for such long a duration.

In order to account for this issue, a short term variability study is performed on each recorded wave spectrum. The numerical model is set up according to the description in Section 3.1, with the viscous damping drag coefficients set to zero. 32 cases are created for each environmental condition, varying the wave seed of each of the 15 directional wave spectra individually. Random wave seeds are created using the Matlab function "Rand", which generates pseudorandom and pseudoindependent numbers. After simulations are completed, the standard deviation of low frequency motion combined surge and sway motion for each case is analysed. The random wave seed which gives the closest result to the mean of all seeds is used for the drag coefficient fitting. An example of the procedure is shown in Figure 1.
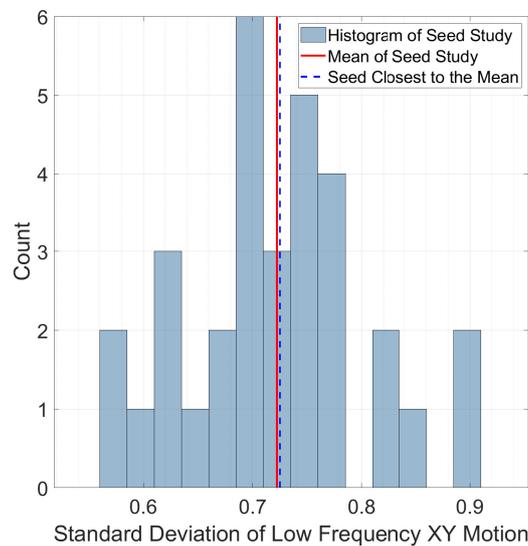
Figure 1: Example of random wave phase seed study for low frequency motions. Note: platform motions have no additional viscous damping here

The drag coefficient will also be fitted to the random wave seeds that give the maximum and minimum motions for one observation point in each group. The single observation point from each of the groups to have this further fitting will be selected randomly.

4. Results

The required drag coefficient are successfully tuned for 64 of the 97 observed data points and are plotted against significant wave height in Figure 2. A failure was found in 33 of the cases, where even with a drag coefficient of zero, the simulated motion was smaller than that observed. In these cases the random wave seed which gave the mean motion was deemed to produce too large motions. No further analysis of these data points was undertaken in this work. In the figure error bars indicate the drag coefficients required to fit to random wave seed which gave the maximum and minimum offsets. The fitted drag coefficients range from almost zero to about 6.5, while no discernible trend correlated with wave height can be observed. The mean of all environmental cases fitted drag coefficient is 1.86. The required drag coefficient for the maximum to minimum random wave seed range can be as small as 0.3 or as large as 3.

Comparisons were made to the drag coefficients resulting from each of the environmental selection criteria, i.e. with or without the wind speed limit of 10 m/s in order to identify if

wind damping was to account for the variance in wave viscous damping. As Figure 2 shows, the variance in drag coefficients for wave heights below 3.5m are similar to those above 3.5m, indicating that wind damping is not a significant cause in this case. A similar comparison to current velocity also showed no correlation to drag coefficient value.

There is little published literature on the surge drag coefficients of advanced spar platforms, however Hirai [22] calculated the required surge drag coefficients for an advanced spar using OpenFOAM CFD. A parameter study on the spars hull diameter found the required drag increased from 1.9 for a pure spar platform to 3.3 for an advanced spar with column to hull ratio of 6. For comparison the column to hull ratio of the advanced spar used in this work is 6.68, but is composed of 2 fully submerged hulls and 1 semi-submerged hull, as opposed to a single fully submerged hull as in Hirai's work

In parallel to this work, the authors have experimentally studied the low frequency surge drag damping of a generic advanced spar platform. Results from these experiments in still water and regular waves indicate a strong KC and wave height/period relationship [23]. The drag coefficients are seen to be inversely proportional to KC number. In that paper the fitted drag coefficients from Figure 2 are plotted against the observed KC number, showing a similar inverse relationship.
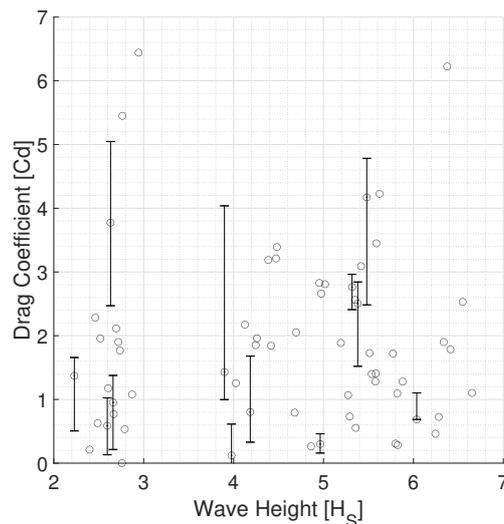
Figure 2: Results of drag coefficients fitted to observation data. Error bars indicate the fit to the max and the min random wave seeds

Wave frequency surge and sway motions are extremely well predicted by all mooring modelling methods used in this work and as discussed in the authors previous research and are not discussed further in this work. Surge/sway natural periods are around 165 s, meaning only around 7 oscillations per are recorded per observation point. In order to further take into account the wave elevation short term variability as described in section 3.2.1, individual observation points are grouped as in the authors previous research [2]. Shown in detail in this work are the groups 8, 12 and 14, details of which are given in table 1.

In Figure 3, cumulative exceedence probabilities are plotted for the three groups, comparing the observed low frequency motions with those simulated by the various mooring models. Results are normalised by the largest motion of the observed data. The standard deviations are shown in an insert bar plot, where error bars indicate the maximum and minimum standard deviation of each group, while the bar indicates the group mean. As the FEM model is tuned to the

Table 1: Grouping data

Group number	Min significant wave height H_S [m]	Max significant wave height H_S [m]	Min peak period T_P [s]	Max Peak Period T_P [s]	Count
8	4.0	4.5	13.00	14.20	9
12	5.5	6.0	11.05	12.20	10
14	5.5	6.0	13.35	14.50	4

observed values, an extremely close fit as seen here is expected. The tails of the distributions are of most interest and significance to the design of such a platform and mooring system, and although drag coefficient values are tuned on the standard deviation of motions, the tails also agree extremely well. For groups 8 and 14, the motion peak is nearly exactly predicted by the FEM model, while for group 12 it shows a 10 % over the observed data.

The analytical catenary models show a slight increase over the FEM model. This difference is attributed mostly due to the lack of viscous mooring line damping applied in this model. In general the difference between the analytical catenary and FEM models grow with increased motions. Both spring methods greatly over predict motions for groups 8 and 14, while show a reasonable prediction for group 12. The linear spring shows a surprising slight improvement over the catenary spring for group 12.

In Figure 4, cumulative exceedance probabilities are given for the fair lead line tensions, again values are normalised by the peak of the observed data. For groups 8 and 12, the shape of all distributions are very similar, although the "observed" values over predict the FEM tensions by about 7-8%. The analytical catenary values over predict the FEM values by about 1-3 %. For group 14, both FEM and the analytical catenary methods give slight over predictions of the observed data of about 3-4 % at the peak. Across all groups the FEM models better predict the sharp increase of tensions at the low probability extreme values more similar to the observed data.

Differences in the FEM model tensions and those from the "observed" analytical catenary data are most likely due to a combination of the following; small changes in the predicted and simulated mean offset, the lack of additional line damping and added mass in the analytical catenary model and lack of line shape effects in the analytical catenary model. It should also be noted that the "observed" values here are from the analytical catenary

5. Conclusions

In this paper, a numerical model of the Fukushima FORWARD floating substation was compared against the observed data recorded in real full scale sea conditions. The required viscous drag coefficient was tuned so as to match the numerical models standard deviation of low frequency surge and sway to the observed data. A large spread in drag coefficients is observed, from almost zero to over six, which is mostly attributed to the short observed time series, where metocean conditions are stable. The mean of all environmental cases fitted drag coefficient is 1.86. With a natural surge frequency of about 165 seconds, these 20 minute observed recordings only give approximately 7 low frequency oscillations. A study to account for the range in required drag coefficients according to wave random phase short term variability also showed a large spread in the required drag coefficients. No trend in the drag coefficients correlated to wave height was observed. However an inverse KC drag coefficient relationship has been observed based on the results from this fitting [23]. The large spread in fitted drag coefficients may also indicate something missing from the numerical model.
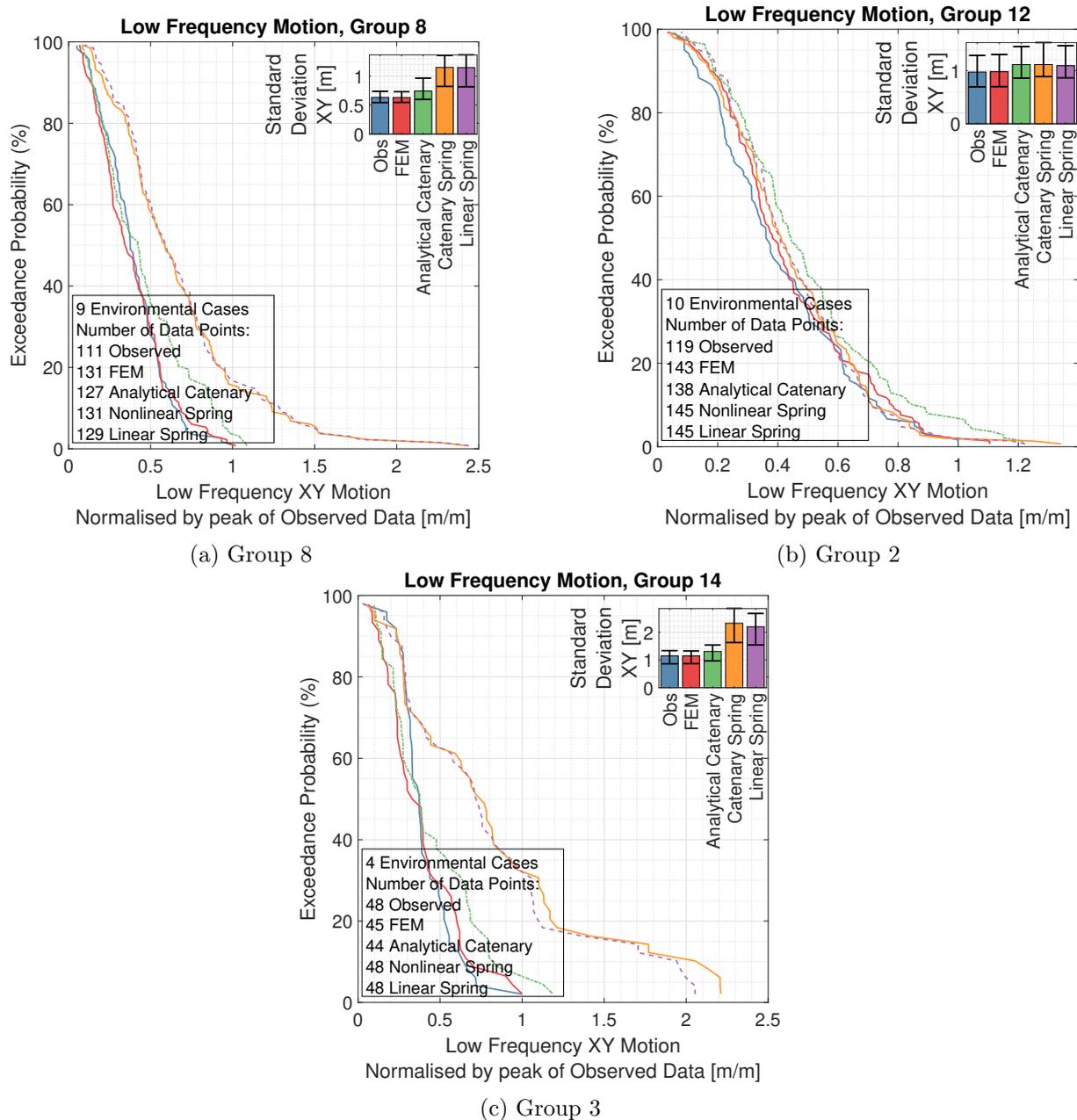
(a) Group 8

(b) Group 2

(c) Group 3

Figure 3: Cumulative exceedance probability and standard deviation of low frequency motions, groups 8, 12 and 14

Various station keeping numerical modelling methods were compared. The extreme tail of the FEM models low frequency motions distribution compared favourably with the observed data. The analytical catenary equation model showed a slight over prediction of the peak data. Generally both spring methods greatly over predicted the peak, by about 2.2-2.5 times, although for a single group, group 12, the spring methods showed consistent results with the observed data, with only the extreme tail showing an over prediction.

As no recorded line tensions are available from the floating substation, the vessels motions are used as input to the analytical catenary model, which result in a quasi-static approximation of the observed loads. Predictions by numerical models are always within 10% of the observed

(a) Group 8

(b) Group 2

(c) Group 3
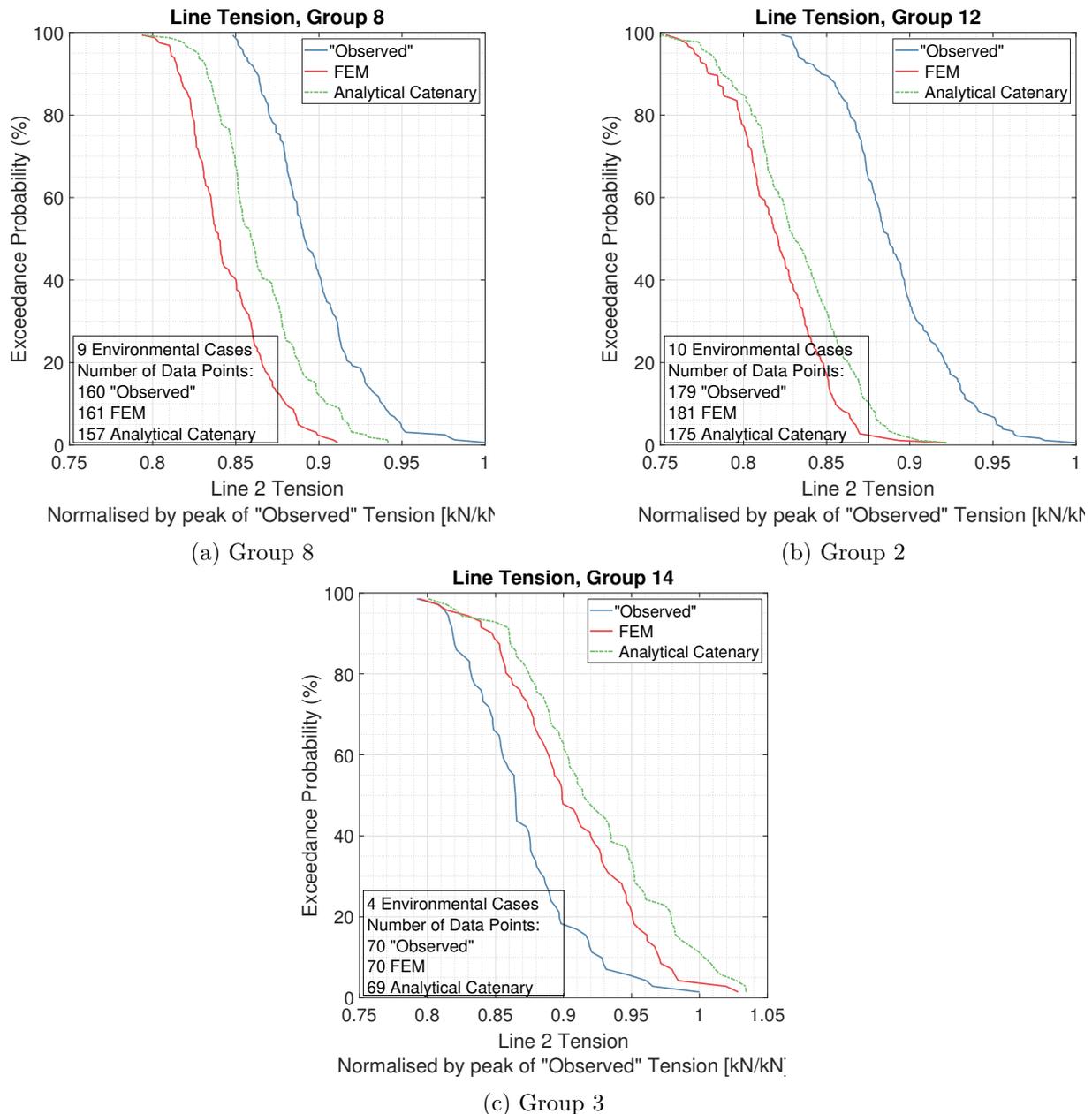
Figure 4: Cumulative exceedance probability and standard deviation of mooring line tensions, groups 8, 12 and 14

values, and in most cases a closer fit is achieved. This work further validates the numerical modelling of the advanced spar floating substation. The use of a quasi-static mooring line model such as the analytical catenary equations here give reasonable results.

References

[1] Jiang Z, Cui J, Gao Y, Liu J and Zhao Y 2016 *Ship Technology Research* **63** 26–37

[2] Wright C, Yoshimoto H, Wada R and Takagi K 2019 Numerical modelling of a relatively small floating body's wave and low frequency motion response, compared with observational data *Proc. ASME 2019 38th Int. Conf. on Ocean, Offshore and Arctic Engineering* (American Society of Mechanical Engineers Digital Collection)

[3] Bhinder M A, Babarit A, Gentaz L and Ferrant P 2015 *Int. J. of Marine Energy* **10** 70–96

[4] Lemmer F, Yu W, Cheng P, Pegalajar-Jurado A, Borg M, Mikkelsen R F and Bredmose H 2018 The triplespar campaign: Validation of a reduced-order simulation model for floating wind turbines *Proc. ASME 2018 37th Int. Conf. on Ocean, Offshore and Arctic Engineering* (American Society of Mechanical Engineers Digital Collection)

[5] Madsen F J, Pegalajar-Jurado A, Bredmose H, Faerron-Guzman R, Müller K and Lemmer F 2015 *LIFE50+ Deliverable D4.6 Model validation against experiments and map of model accuracy across load cases*

[6] Pegalajar-Jurado A and Bredmose H 2019 *Marine Structures* **66** 178–96

[7] Faltinsen O 1993 *Sea Loads on Ships and Offshore Structures* vol 1 (Cambridge: Cambridge university press)

[8] Ishihara T and Zhang S 2019 *Renewable energy* **131** 1186–207

[9] Stansberg C T, Kaasen K E, Abrahamsen B C, Nestegård A, Shao Y, Larsen K *et al.* 2015 Challenges in wave force modelling for mooring design in high seas *Offshore Technology Conference* (Offshore Technology Conference)

[10] Yang L, Falkenberg E, Nestegård A and Birknes-Berg J 2017 Viscous drift force and motion analysis of semi-submersible in storm sea states compared with model tests *Proc. ASME 2017 36th Int. Conf. on Ocean, Offshore and Arctic Engineering* (American Society of Mechanical Engineers Digital Collection)

[11] Fonseca N and Stansberg C T 2017 Wave drift forces and low frequency damping on the exwave fpso *Proc. ASME 2017 36th Int. Conf. on Ocean, Offshore and Arctic Engineering* (American Society of Mechanical Engineers Digital Collection)

[12] Prislin I, Halkyard J, DeBord F, Collins J I, Lewis J M *et al.* 1999 Full-scale measurements of the oryx neptune production spar platform performance *Offshore Technology Conference* (Offshore Technology Conference)

[13] Saito M, Kato S, Ohkawa Y *et al.* 1993 Free decaying test and simulation of slow drift motion of prototype floating structure" poseidon" *The Third International Offshore and Polar Engineering Conference* (International Society of Offshore and Polar Engineers)

[14] Driscoll F, Jonkman J, Robertson A, Sirnivas S, Skaare B and Nielsen F G 2016 *Energy Procedia* **94**

[15] Yoshimoto H, Yoshida H and Kamizawa K 2018 Validation of applicability of low frequency motion analysis theory using observation data of floating offshore substation *ASME 2018 37th International Conference on Ocean, Offshore and Arctic Engineering* (American Society of Mechanical Engineers Digital Collection)

[16] Yoshimoto H and Kamizawa K 2019 Validation of the motion analysis method of floating offshore wind turbines using observation data acquired by full scale demonstration project *International Conference on Offshore Mechanics and Arctic Engineering* (American Society of Mechanical Engineers)

[17] Nakamura A, Hayashi Y and Ichinose H 2018 Verification of load calculation based on site measurements of a 7mw offshore wind turbine on v-shaped semi-submersible floating structure *Grand Renewable Energy proceedings Japan council for Renewable Energy* (Japan Council for Renewable Energy)

[18] Komatsu M, Mori H, Tanaka H, Ohta M, Karikomi K and Ishii H 2018 Comparison between measured value and simulated value of motion and mooring force in mitsubishi 7mw floating offshore wind turbine *Grand Renewable Energy proceedings Japan council for Renewable Energy* (Japan Council for Renewable Energy)

[19] Stansberg C T and Gudmestad O T 1996 Non-linear random wave kinematics models verified against measurements in steep waves Tech. rep. American Society of Mechanical Engineers, New York, NY (United States)

[20] OCIMF 1994 Prediction of wind and current loads on vlccs (Oil Companies International Marine Forum London)

[21] Berthelsen P A, Bachynski E E, Karimirad M and Thys M 2016 Real-time hybrid model tests of a braceless semi-submersible wind turbine: Part iii—calibration of a numerical model *Proc. ASME 2016 35th Int. Conf. on Ocean, Offshore and Arctic Engineering* (American Society of Mechanical Engineers Digital Collection)

[22] Hirai T, Sou A and Nihei Y 2018 Wave load acting on advanced spar in regular waves *Proc. ASME 2018 37th Int. Conf. on Ocean, Offshore and Arctic Engineering* (American Society of Mechanical Engineers Digital Collection)

[23] Wright C, Yoshimoto H, Wada R and Takagi K 2020 Experimental identification of an advanced spar's low frequency drag damping in waves *Proc. ASME 2020 39th Int. Conf. on Ocean, Offshore and Arctic Engineering* (American Society of Mechanical Engineers Digital Collection)